Cell, Vol. 102, 99–108, July 7, 2000, Copyright ©2000 by Cell Press

Structural Basis for the Interaction between FxFG Nucleoporin Repeats and Importin-β in Nuclear Trafficking

Richard Bayliss, Trevor Littlewood, and Murray Stewart*
MRC Laboratory of Molecular Biology
Cambridge CB2 2QH
United Kingdom

Summary

We describe the crystal structure of a complex between importin-β residues 1–442 (Ib442) and five FxFG nucleoporin repeats from Nsp1p. Nucleoporin FxFG cores bind on the convex face of Ib442 to a primary site between the A helices of HEAT repeats 5 and 6, and to a secondary site between HEAT repeats 6 and 7. Mutations at importin-β Ile178 in the primary FxFG binding site reduce both binding and nuclear protein import, providing direct evidence for the functional significance of the importin-β–FxFG interaction. The FxFG binding sites on importin-β do not overlap with the RanGTP binding site. Instead, RanGTP may release importin-β from FxFG nucleoporins by generating a conformational change that alters the structure of the FxFG binding site.

Introduction

The bidirectional transport of macromolecules between the cytoplasm and nucleus through nuclear pore complexes (NPCs) is mediated by shuttling transport factors or carrier molecules that bind their cargo in one compartment and release it in the other (reviewed by Adam, 1999; Görlich and Kutay, 1999; Nakielny and Dreyfuss, 1999; Stewart and Rhodes, 1999; Talcott and Moore, 1999). Carrier molecules are primarily members of the importin-β/karyopherin-β superfamily and the interaction with their cargo is orchestrated by the nucleotide state of the Ran GTPase (reviewed by Görlich, 1998; Melchior and Gerace, 1998). For example, in nuclear protein import, cargo molecules bind to importin-β in the cytoplasm (where Ran is thought to be primarily in the GDP-bound form), either directly or via an adaptor such as importin-α, whereas RanGTP dissociates the cargo-carrier complex in the nucleus. Translocation of the carrier-cargo complex from the cytoplasm to the nucleus takes place along the central axis of the NPC (Feldherr et al., 1984) and involves interactions with nucleoporins (NPC proteins) that contain characteristic Phe-rich repeating sequence motifs (Radu et al., 1995a, 1995b; Rexach and Blobel, 1995; Chi and Adam, 1997; Hu et al., 1997; Shah and Forbes, 1998; Kose et al., 1999; Seedorf et al., 1999; Yaseem and Blobel, 1999; Damelin and Silver, 2000). Crystallographic studies have defined the interactions between RanGTP, importin-β, and importin-α that are fundamental to nuclear trafficking (Cingolani et al., 1999; Chook and Blobel, 1999; Vetter et al., 1999), but the nature of the interaction between importin-β and nucleoporins and the way in which RanGTP dissociates this interaction are less clear.

The crystal structures of importin-β and its close homolog, karyopherin-β2, bound to RanGTP or the importin-α IBB domain (importin-β binding domain) have been determined (Cingolani et al., 1999; Chook and Blobel, 1999; Vetter et al., 1999). Importin-β is constructed from 19 tandem "HEAT" sequence repeats, each containing approximately 40 residues and constructed from an A and a B helix connected by a short turn. The HEAT repeats are joined by a short linker and are arranged to produce a right-handed superhelical molecule in which the A helices are located primarily on the outer, convex surface, whereas the B helices are located on the inner, concave surface (Cingolani et al., 1999; Chook and Blobel, 1999; Vetter et al., 1999). RanGTP and the IBB domain bind to extensive sites located primarily on the inner face of importin-β. The IBB domain interacts with HEAT repeats 7–19 (Cingolani et al., 1999), whereas RanGTP interacts with HEAT repeats 1–3, 6, 7, 13, and 14 (Chook and Blobel, 1999; Vetter et al., 1999).

Many of the proteins from which NPCs are constructed (nucleoporins) contain tandem sequence repeats based on cores containing Phe and Gly separated by linkers of variable sequence and length that are rich in hydrophilic residues. Two common core motifs are FxFG and GLFG (Rout and Wente, 1994; Rout et al., 2000). A number of lines of evidence indicate that these nucleoporins have a role in nuclear trafficking. Nuclei reconstituted in *Xenopus* egg extracts depleted of nucleoporins that bind wheat germ agglutinin (WGA) are deficient in nuclear protein import, but transport is restored by addition of these nucleoporins (Finlay and Forbes, 1990). Interactions between members of the importin-β family and nucleoporin repeats have been shown in vitro (for example, Radu et al., 1995a, 1995b; Rexach and Blobel, 1995; Chi and Adam, 1997; Hu et al., 1997; Shah et al., 1998; Kose et al., 1999; Seedorf et al., 1999; Kehlenbach et al., 1999) and in vivo (Damelin and Silver, 2000). In the case of nuclear protein import mediated by importin-β, an interaction between importin-β and Nup358 is probably involved in the initial docking step (Yaseem and Blobel, 1999), whereas the terminal step of transport appears to be the release of the importin-substrate complex from the FxFG repeat-containing region of Nup153 by RanGTP (Görlich et al., 1996; Shah et al., 1998; Shah and Forbes, 1998). Both the translocation of the importin–substrate complex through the NPC and the subsequent recycling of importin-β to the cytoplasm are also thought to involve interactions between FxFG nucleoporins and importin-β (Rexach and Blobel, 1995; Kose et al., 1999). The strength of the interaction between different FxFG nucleoporins and importin-β appears to vary. Thus, although an interaction between importin-β and Nup62 is seen in solution binding studies (Hu et al., 1997) and blot overlays (Bonifaci et al., 1997), it is not detected in

*To whom correspondence should be addressed (e-mail: ms@mrc-lmb.cam.ac.uk).

Xenopus egg extracts, either because it is too weak or because the interaction site on Nup62 is masked, whereas the Nup153–importin-β interaction is easily detected (Shah et al., 1998). Different members of the importin-β family show different patterns of interaction with different repeat-containing nucleoporins that are modulated by RanGTP (see, for example, Seedorf et al., 1999; Kehlenbach et al., 1999). FxFG nucleoporins are located at the cytoplasmic and nucleoplasmic faces of the NPCs (reviewed by Stoffler et al., 1999; Rout et al., 2000) and also line the central channel (Grote et al., 1995). Studies using importin-β truncation mutants indicate that the binding site for FxFG repeat nucleoporins is located in the N-terminal half between residues 152 and 352 (Chi and Adam, 1997; Kutay et al., 1997; Kose et al., 1999). In addition to importin-β family members, FxFG nucleoporin repeats also bind NTF2 (Paschal and Gerace, 1995; Clarkson et al., 1996, 1997) and this interaction mediates the nuclear import of RanGDP (Bayliss et al., 1999).

Here, we describe the crystal structure of a complex formed between residues 1–442 of importin-β (Ib442) and a construct containing five tandem FxFG repeats from nucleoporin Nsp1p (FF5). The FxFG cores of FF5 bind on the convex face of Ib442 at a primary site located between the A helices of HEAT repeats 5 and 6 and at a secondary site between the A helices of HEAT repeats 6 and 7. Neither site overlaps the RanGTP binding site and RanGTP may release importin-β from the nucleoporin repeats by generating a conformational change that moves the A helix of HEAT repeat 5 relative to repeat 6, thereby occluding the interaction site. Mutations at Ile178, a key component of the primary importin-β FxFG binding site, decrease the binding of FxFG nucleoporins and also result in reduced levels of nuclear protein import in permeabilized cells.

Results and Discussion

Structure of the Ib442-FxFG Repeat Complex

Although small crystals were obtained using several combinations of constructs of importin-β with nucleoporin repeats or synthetic peptides, crystals suitable for high-resolution analysis were obtained only from Ib442 (residues 1–442 of human importin-β corresponding to HEAT repeats 1–10) and FF5 (residues 497–608 of yeast Nsp1p). Previous studies (Seedorf et al., 1999) showed an interaction in vivo between the yeast importin-β homolog Kap95 and Nsp1p and several other nucleoporins. FF5 contained five FxFG repeats in which the linkers are highly conserved (Figure 1D). The CD spectrum of FF5 showed little absorption above 210 nm and a large minimum at 200 nm, indicating that it had little regular secondary structure in solution (Greenfield and Fasman, 1969). Several other Nsp1p FxFG constructs (Clarkson et al., 1996) showed a similar CD spectrum and yet were able to bind to both importin-β and NTF2, indicating that the interaction between transport factors and the FxFG nucleoporin repeats was not critically dependent on the repeats adopting a defined structural fold in solution (although a defined fold may be induced by binding). Flexibility of the FxFG repeats would also be consistent with the somewhat diffuse localization within NPCs observed for many nucleoporins (Stoffler et al., 1999; Rout et al., 2000).

The structure of the Ib442–FF5 complex was determined by molecular replacement. We located two Ib442 chains in the asymmetric unit using residues 1–442 of importin-β bound to the IBB domain (Cingolani et al., 1999) as a model. After rigid body and group B factor refinement, the R factor of the molecular replacement solution was 29.8% (R_{free} 31.5%) which simulated annealing reduced to 25.1% (R_{free} 28.3%). Although there was no F_o-F_c difference density indicative of a third Ib442 chain, both the $2F_o-F_c$ electron density map obtained after solvent flipping and the F_o-F_c difference density map showed two distinct tubes of density on the convex surface of both Ib442 chains. The more distinct of these tubes, which we refer to as the primary site, was located between the A helices of HEAT 5 and HEAT 6 (red and green in Figures 1A and 1B), whereas the less distinct secondary site density was between the A helices of HEAT 6 and HEAT 7 (green and blue in Figures 1A and 1B). Both Ib442 chains in the asymmetric unit showed the same pattern of difference density on their surface and, in particular, each primary site showed two large protrusions consistent with the presence of the two Phe side chains of the FxFG repeat core. After iterative cycles of fitting the sequence of the Nsp1p repeats to the density, followed by simulated annealing of the repeat sequence, the R factor was reduced to 22.5% (R_{free} 26.2%). The final structural model (Table 1) contained residues 1–440 of Ib442 and two separate stretches of nucleoporin repeat (13 residues for the primary site and 8 for the secondary site). Figure 1B illustrates the FF5 cores (yellow) that could be built reliably, whereas Figure 2 shows a portion of the final $2F_o-F_c$ electron density map near the FxFG core at the primary site. As one moved along the FF5 chain away from the regions bound to Ib442, the density became less well defined, the B factors for the atoms increased above 100 $Å^2$, and the path of the chain became difficult to trace unequivocally. It was therefore not possible to establish the precise connectivity between the FxFG cores at the two binding sites or to know whether the FF5 chain could link Ib442 chains in the crystal. The diffuse FF5 electron density distant from the binding sites on Ib442 was consistent with the CD data, indicating that the FF5 construct did not contain a large amount of regular structure and so was able to assume a number of alternate conformations. Under these conditions, only the residues directly interacting with the Ib442 construct would be strongly constrained and so give rise to clear electron density. Residues further from the binding site would, because of the flexibility of FF5, take up a range of different positions which would be averaged in the electron density map and so would appear only as diffuse density. Although we were not able to trace the full FF5 chain, it was well defined in the regions in contact with Ib442 (Figure 2) and therefore the location of the binding site in Ib442 and the central role of the FxFG core was unequivocal. The observation that the interaction with importin-β involved primarily the cores of the FF5 repeats was consistent with the observation that a range of different FxFG nucleoporins bind to transport

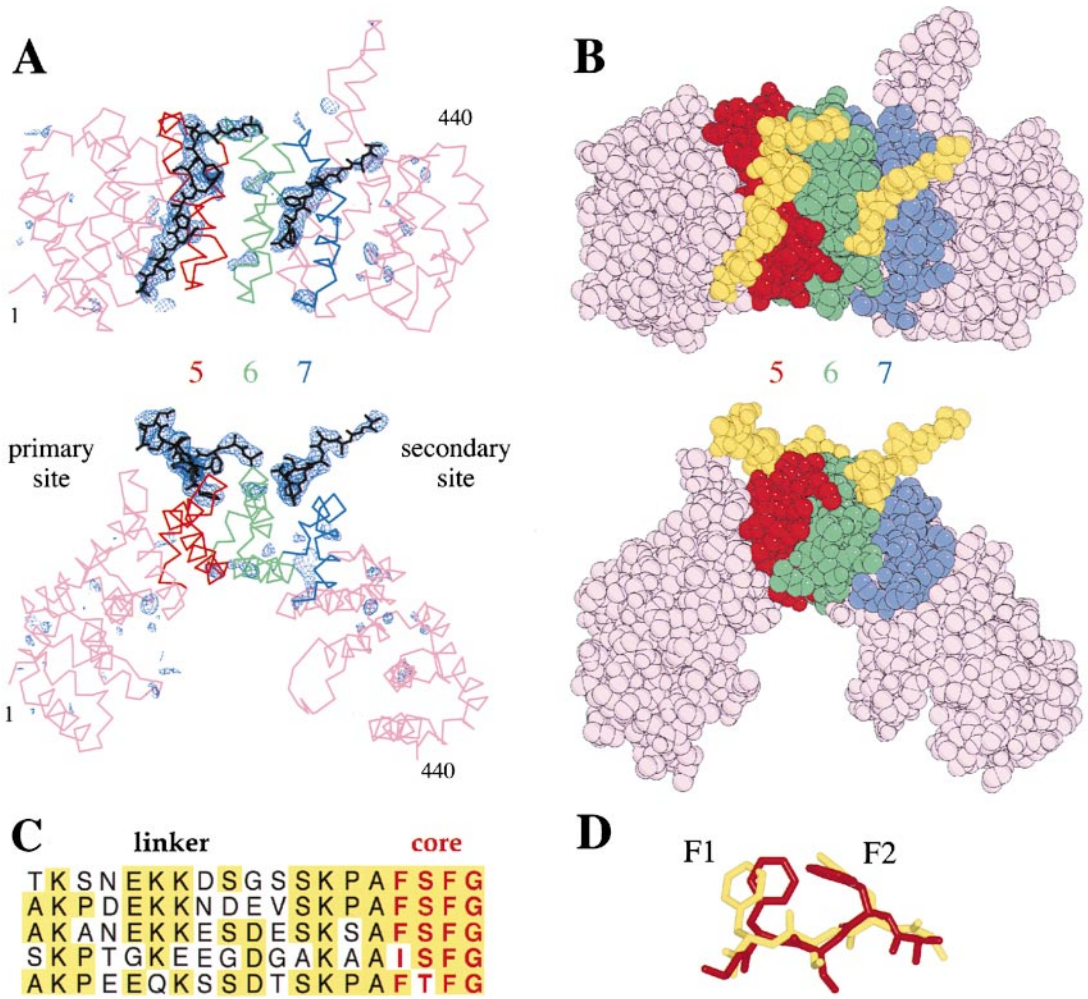

Figure 1. FxFG Nucleoporin Repeats Bind to the Convex Surface of Importin-β 1–442

(A) Annealed omit electron density map showing the tubes of density due to the nucleoporin FxFG repeats observed on the convex surface of the 1–442 construct of importin-β (Ib442). HEAT repeats 5, 6, and 7 of importin-β are shown as red, green, and blue whereas the model built for the nucleoporin repeats is black. The density between HEAT repeats 5 and 6 was more distinct and is referred to as the primary site, whereas the less distinct difference density between HEAT repeats 6 and 7 is referred to as the secondary site. The map is contoured at 3 σ and shows the A chain in the asymmetric unit.

(B) cpk model showing the Nsp1p FxFG repeats (yellow) bound to the outer, convex surface of Ib442.

(C) Sequence of FF5 (Nsp1p residues 497–608), which contains five cores based on the sequence FSFG separated by highly conserved 15-residue hydrophilic linkers.

(D) Structural conservation between FxFG repeat cores. Superposition of the FxFG cores at the primary (red) and secondary (yellow) sites on Ib442 illustrating how they have similar folds, with the Phe sidechains (F1 and F2) taking up similar conformations.

factors (Rexach and Blobel, 1995; Hu et al., 1997; Bonifaci et al., 1997; Seedorf et al., 1999) even though the length and sequence of the linkers varies considerably both within and between nucleoporins (see Rout and Wente, 1994; Clarkson et al., 1996).

The conformation taken up by the FxFG cores was similar between secondary and primary sites (Figure 1D). In both, the polypeptide chain approximated a β strand with a core Cα rmsd of 0.58 Å. Although there was a small variation in sidechain orientation, both cores showed an analogous stacking of Phe sidechains. Although it was not possible to determine whether the cores had a similar conformation in solution, the primary and secondary binding sites on importin-β were somewhat different, making it less likely that the conformation of the FxFG cores was induced by the interaction. The interaction seen between Phes in each core might help retain this conformation in solution and the small quantity of β conformation in the core would not be easily detected by CD if the linkers were flexible.

Binding Sites on Ib442 for FxFG Repeats

The interactions between FF5 and the primary site on Ib442 involved almost exclusively the two Phes of the FxFG core (yellow in Figures 3A and 3B), which were buried in a hydrophobic pocket generated by sidechains from the A helices of HEAT repeats 5 and 6 (blue). The second Phe of the core (F2) made a greater contribution to the interface and buried parts of the sidechains of

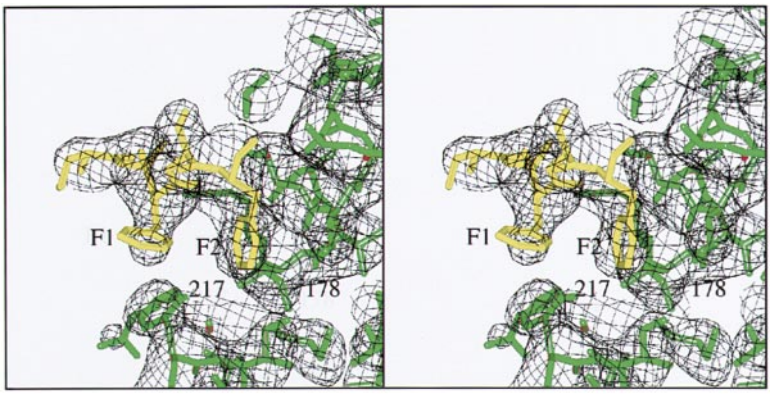

Figure 2. Electron Density at the Primary FxFG Binding Site on Importin-β 1–442

Stereo view of the final σ_A-weighted $2F_o-F_c$ electron density map near the primary FxFG binding site on importin-β 1–442 between the A helices of HEAT repeats 5 and 6. The importin-β chain is green and the Nsp1p FxFG repeat chain is yellow.

Leu174, Thr175, Ile178, Glu214, Phe217, and Ile218 of Ib442, although the first Phe (F1) formed a good stacking interaction with the ring of Phe217. In addition to the Ib442 residues buried by interaction with the FxFG core, the Phes of the core stacked against one another (Figure 1D) contributing to the surface buried. Approximately 670 Å^2 of surface area was buried by the cores (677 Å^2 for chain A and 663 Å^2 for chain B) whereas approximately 1000 Å^2 was buried by the entire primary site (1041 Å^2 for chain A and 971 Å^2 for chain B). The residues on importin-β involved in the interaction are not strictly conserved between species, but substitutions at these positions are conservative (Figure 3C) and should not interfere with binding to the FxFG core. Glu214 is the only strictly conserved residue involved in the interaction. The aliphatic part of its sidechain forms part of the hydrophobic pocket which binds F2, and its acid group is well positioned to form an H bond with the mainchain N of the FxFG core Gly.

A putative secondary binding site for FxFG repeats was located between the A helices of HEAT repeats 6 and 7 (Figures 1A and 1B). The chain tracing at this site was not as clear as for the primary site, the B factors were higher, and the surface area buried was 500–600 Å^2, although the FxFG core adopted similar conformation to that at the primary site (Figure 1D). Again, the interaction with Ib442 was primarily hydrophobic and involved aromatic stacking of F1 onto conserved Tyr255 and also F1 burying the sidechain of Pro258, together with the aliphatic regions of Gln220 and His216. The sidechain of F2 was buried in a pocket composed of the aliphatic regions of Glu224, Ala259, and Cys223. Although the binding of the FxFG core to the secondary site may have been facilitated by the repeat being already bound to

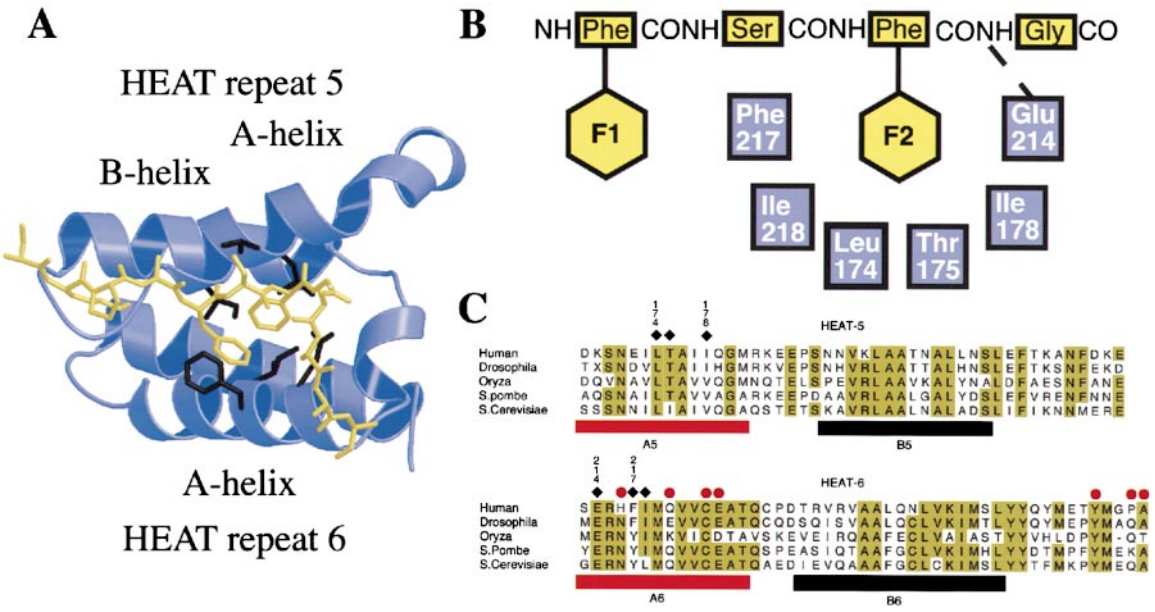

Figure 3. Interactions at the Primary FxFG Nucleoporin Biding Site on Importin-β 1–442

(A) View of the primary FxFG nucleoporin binding site on importin-β showing how a repeat core (yellow) interacts with key residues (black) in the A helices of HEAT repeats 5 and 6.

(B) Schematic of the importin-β residues that interact with the FxFG core at the primary site.

(C) Conservation of key residues in HEAT repeats 5 and 6 between different species at both the primary (diamond) and secondary (circle) sites.

the primary site, the observation that modification of Cys223 and Cys228 interfered with the binding of importin-β to NPCs (Chi and Adam, 1997) suggests that this site may be functionally significant.

The structure of the Ib442–FF5 complex shows that both the primary and secondary FxFG binding sites were on the outer convex surface of the importin-β molecule (Figures 1A and 1B) and so are ideally placed to interact with nucleoporins during transport. By contrast, the binding sites for cargo such as the importin-α IBB domain are on the inner concave surface and enveloped by importin-β (see Cingolani et al., 1999). This disposition of binding sites would account for importin-β binding both FxFG repeats and substrates such as the IBB domain simultaneously (e.g., Radu et al., 1995a), which would be important if the FxFG nucleoporins were to function as docking sites for the translocation of the cargo–carrier complex through NPCs.

Mutants That Reduce Importin-β Binding to FxFG Repeats Reduce Nuclear Protein Import

Engineered point mutants confirmed that the primary FxFG binding site on Ib442 observed in the crystal structure was important for binding full-length importin-β to FxFG nucleoporins. Ile178, which forms part of the hydrophobic pocket between the A helices of HEAT 5 and HEAT 6, was mutated to Ala (increasing the size of the pocket), Phe (decreasing the size of the pocket to sterically hinder FxFG core binding), or Asp (to make the site less hydrophobic). Wild-type importin-β and the mutants all bound RanGTP and importin-α to comparable levels (Figure 4A). Because both the importin-α IBB domain and RanGTP interact at a number of sites on importin-β (Cingolani et al., 1999; Vetter et al., 1999), this was a powerful positive control indicating that the mutants had folded correctly. To test the binding to FxFG repeats, we employed both solution binding and blot-overlay assays. In solution, the Ile178 mutants bound to FF5 (the yeast Nsp1p construct containing five FxFG repeats) linked to Sepharose much less strongly than wild-type importin-β (Figure 4A). We used blot overlays to assess the binding of the importin-β mutants to vertebrate nucleoporins. Previous studies (Finlay and Forbes, 1990; Radu et al., 1995a; Bonifaci et al., 1997) showed that extracts of rat nuclear envelopes prepared using WGA-affinity chromatography contain four FxFG nucleoporins (Nups 62, 153, 214, and 358) that are recognized by monoclonal antibody MAb414 together with the GLFG-nucleoporin Nup98, and that importin-β binds to all these nucleoporins in blot overlays. We observed a similar pattern using S-tagged wild-type importin-β, with strong bands corresponding to NUP62, NUP98, and NUP153 and weaker bands for Nup214 and Nup358 (Figure 4B, lane 2). Moreover, the binding of importin-β to Nups 62, 153, 214 and 358 was competed by the Nsp1p FxFG construct FF18 (Figure 4B, lane 3), consistent with FxFG repeats being important for the interaction. Significantly, the binding to Nup98, which contains primarily GLFG repeats (Radu et al., 1995b), was not competed by FF18. The importin-β Ile178 mutants (Figure 4B, lanes 4–6) retained binding to NUP98, but showed reduced binding to the rat FxFG nucleoporins, with I178F and I178D showing virtually no binding and

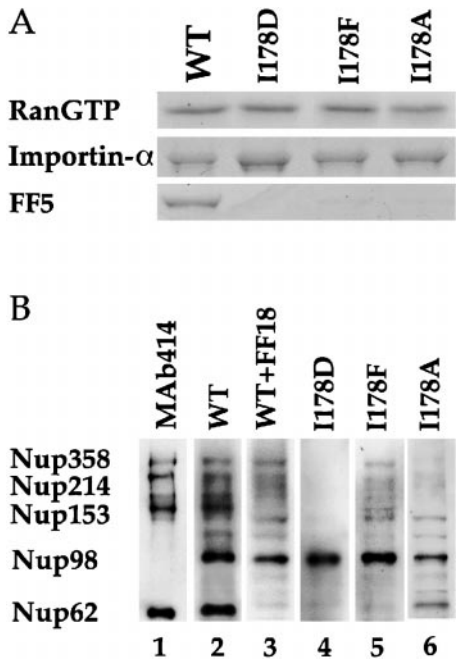

Figure 4. Importin-β Ile178 Mutants Bind Less Strongly to FxFG Repeats

(A) Solution binding. S-tagged wild-type importin-β and the Ile178 mutants all bound RanGTP and importin-α to comparable levels, indicating that the mutations had not introduced a major conformational change. Wild-type importin-β bound to five repeats (FF5) of yeast Nsp1p whereas the I178A, I178D, and I78F mutants showed much lower levels of binding under the same conditions. (B) Blot overlay assays using a rat liver nuclear envelope extract enriched in FxFG nucleoporins. Wild-type importin-β (lane 2) binds to five bands (see Bonifaci et al., 1997). Monoclonal antibody MAb414 (lane 1) identifies four of these bands as the FxFG Nups 62, 153, 214, and 358 while the remaining strong band is Nup98 (Bonifaci et al., 1997). As observed in previous studies (e.g., Bonifaci et al., 1997), Nups 62, 98, and 153 gave much stronger bands than Nups 214 and 358. Importin-β was displaced from all but Nup98 (which contains GLFG rather than FxFG repeats) by the 18 FxFG repeat construct of Nsp1p (lane 3), confirming that the binding to Nups 62, 153, 214, and 358 involves a major contribution from FxFG repeats. The Ile178 importin-β mutants retained binding to Nup98 but showed greatly reduced binding to the FxFG nucleoporins, which was most marked with I178D (lane 4) and I178F (lane 5), but still clear with I178A (lane 6). These data are consistent with I178 making a major contribution to the FxFG core binding site on importin-β, but with GLFG nucleoporins binding to a different site.

I178A showing very much lower levels of binding than wild type, consistent with the results obtained in solution. In summary, solution binding and blot-overlay assays using the Ile178 mutants were consistent with location of the primary binding site for FxFG cores identified by crystallography (Figures 1 and 3) and with this site being important for the interaction of full-length importin-β with FxFG nucleoporins.

The importin-β Ile178 mutants that showed reduced binding to FxFG repeats also showed reduced levels of nuclear protein import in digitonin-permeabilized HeLa cells (Figure 5). Wild-type importin-β at a concentration of 250 nM showed efficient nuclear import of a fluorescein-labeled NLS-BSA conjugate (Görlich et al., 1996), whereas both the I178D and I178F mutants at the same

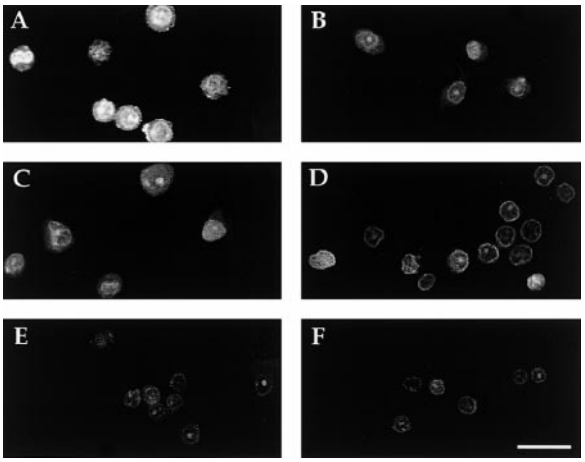

Figure 5. Importin-β Mutants with Reduced FxFG Repeat Binding Show Reduced Levels of Nuclear Protein Import

Importin-β (A) produced a clear accumulation of fluorescent substrate in the bulk of the nucleoplasm of digitonin-permeabilized HeLa cells, whereas the I178D (B) and I178F (C) importin-β mutants showed only weak perinuclear and nucleolar staining, consistent with a reduced rate of nuclear protein import, and I178A (D) gave slightly higher levels of transport but was still much less efficient than wild type. Addition of the FF18 (E) or FF5 (F) constructs containing respectively 18 and 5 Nsp1p FxFG repeats inhibited nuclear protein import by wild-type importin-β. Bar is 25 μm.

concentration showed predominantly weak perinuclear and nucleolar staining with little accumulation of the labeled substrate in the bulk of the nucleoplasm and I178A showed a slightly higher level of import, but was still much less efficient than wild type. The mutant importin-β constructs showed only 16% (I178D) and 12% (I178F) of the level of cells with strong nuclear staining compared with wild-type importin-β, whereas I178A showed 24%. Nuclear import was also inhibited by addition of the yeast Nsp1p FF18 and FF5 FxFG constructs (Figures 5E and 5F) analogous to that seen with FxFG-containing constructs of Nup153 (Shah and Forbes, 1998) and confirming the importance of a general interaction between importin-β and FxFG nucleoporins. No nuclear import was seen in the absence of importin-β nor with a defective NLS conjugate. The reduced import seen with the mutants provided direct evidence for the importance of an interaction between importin-β and FxFG repeats during nuclear protein import, consistent with earlier observations demonstrating these interactions in vivo and in vitro (e.g., Rexach and Blobel, 1995; Chi and Adam, 1997; Hu et al., 1997; Shah and Forbes, 1998; Damelin and Silver, 2000). The requirement for an interaction between FxFG repeats and importin-β during nuclear protein import is analogous to the requirement for an interaction between NTF2 and these repeats during the nuclear import of RanGDP (Bayliss et al., 1999).

Release of Importin-β from FxFG Repeats by RanGTP

A number of studies have indicated that importin-β is released from FxFG nucleoporins by RanGTP (e.g., Rexach and Blobel, 1995; Görlich et al., 1996; Shah and Forbes, 1998). The FxFG and RanGTP binding sites on

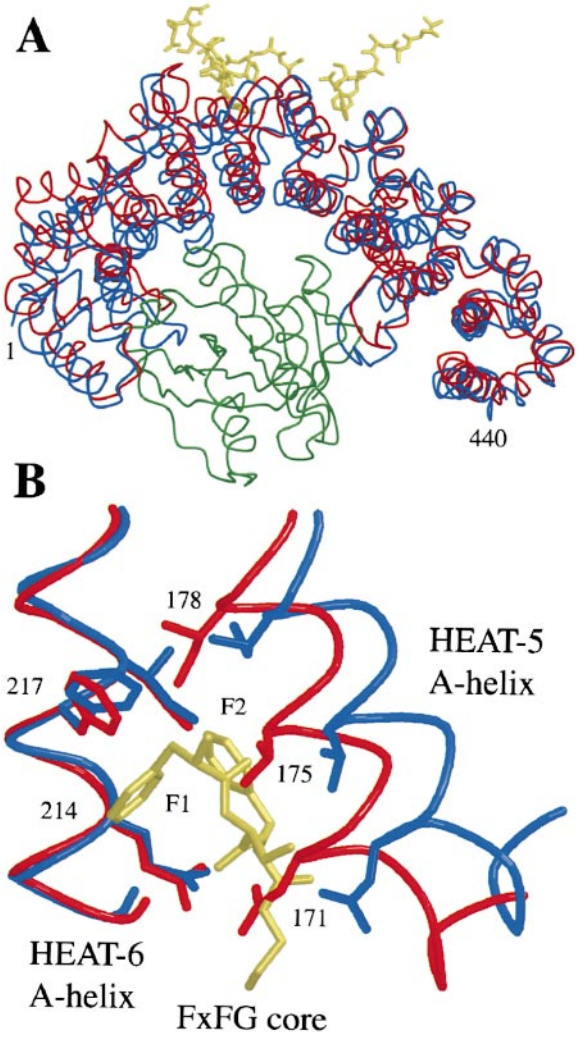

Figure 6. Structural Differences between Importin-β Residues 1–440 Bound to RanGTP or FF5 Suggest How RanGTP May Release Importin-β Bound to FxFG Nucleoporins

(A) Superimposed Cα traces of the importin-β-RanGTP complex (Vetter et al., 1999) and that of the importin-β-1–442/Nsp1p–FxFG repeats complex (Ib442–FF5). The importin-β chain is colored red for Ib442 and blue for the importin-β-RanGTP complex, whereas the Ran chain is green and FxFG repeats are yellow. Compared with the Ib442–FF5 structure, importin-β bound to RanGTP shows a relative movement of successive HEAT repeats.

(B) Movement of helix A of HEAT repeat 5 in importin-β–RanGTP compared with Ib442–FF5. In the Ib442–FF5 structure (red), the sidechains of Phe217, Ile178, and Leu174 of importin-β make key contributions to the primary binding site for the FxFG core (yellow). In the importin-β–RanGTP structure (blue), the A helix of HEAT repeat 5 moves relative to HEAT repeat 6 so that Asn 171, Leu174, and Ile178 move towards Phe217 and obstruct the binding of the two Phe sidechains of the FxFG core.

importin-β do not overlap (Figure 6), suggesting that this displacement is not effected by simple competition of RanGTP and FxFG nucleoporins for the same site. However, comparison of the structure of importin-β in different crystals suggests that this release might be mediated by a conformational change associated with binding RanGTP. Importin-β is flexible, with the superhelical path followed by the HEAT repeats varying between different crystal forms and also between different

Table 1. Crystallographic Data for Ib442–FF5 Crystals

Lattice constants (Å)	a = 67.25	b = 211.79	c = 125.82
Data collection			
Resolution range (Å)‡	40–2.8 (2.95–2.80)		
Number of observations	144382	Number of unique reflections	31295
Completeness‡	40–3.4Å: 98.5%	40–3.2Å: 92.4%	40–2.8Å: 69.1%
Multiplicity‡	4.9 (2.8)	R_{merge} (%)†‡ 8.9 (18.3)	I/σ‡ 6.0 (1.7)
Refinement			
Resolution range (Å)	40–2.8	Number of residues 922	
R factor*	22.5%	R_{free}§ 26.2%	
Bond length rms	0.009 Å	Bond angle rms 1.5°	
Ramachandran plot			
Most favored 88.7%	Allowed 9.5%	Generously allowed 1.4%	Forbidden 0%

‡ Highest resolution shell in parenthesis.
† $R_{merge} = \Sigma_{hkl} \Sigma_i |I_{hkl} - <I_{hkl}>| / \Sigma_{hkl} \Sigma_i <I_{hkl}>$ where $<I_{hkl}>$ is the mean of the observations $I_{hkl,i}$ of reflection *hkl*.
* R-factor $= 100 \times \Sigma_{hkl}[|F_o(hkl)| - |F_c(hkl)|] / \Sigma_{hkl}|F_o(hkl)|$ where F_o and F_c are the observed and calculated structure factors, respectively.
§ Free R was computed using 10% of the data assigned randomly.

chains in the asymmetric unit of the same crystal (Chook and Blobel, 1999; Cingolani et al., 1999; Vetter et al., 1999). The Ib442–FF5 and IBB–importin-β (PDB 1qgk, Cingolani et al., 1999) complex structures were more similar to one another than to importin-β bound to RanGTP (PDB 1ibr, Vetter et al., 1999). The rms Cα difference between the two chains in the Ib442–FF5 complex crystals compared to the IBB–importin-β structure was 1.3 and 2.1 Å. Although this was greater than the differences between the two chains in the Ib442–FF5 crystals (0.7 Å) or that between the corresponding residues in the two IBB–importin-β crystals (0.6 Å), inspection of the structures indicated that this reflected mainly the flexibility of importin-β and crystal packing rather than systematic differences in conformation. The similarity between the crystal structures of Ib442–FF5 and IBB–importin-β indicated that FxFG binding does not introduce a large conformational change in importin-β, consistent with its binding IBB and FxFG nucleoporins simultaneously. The rms differences between these structures were substantially less than those between the Ib442 chains and residues 2–440 of importin-β bound to RanGTP (3.0 Å and 3.4 Å), and there was a more marked difference in the superhelical pitch followed by the HEAT repeats between importin-β complexed with RanGTP compared with importin-β complexed with either the IBB domain or FF5 (Figure 6A). Moreover, the change in the superhelical path with RanGTP was accommodated by substantial movement of some HEAT repeats relative to one another. In particular, when RanGTP was bound to importin-β, there was a substantial movement of the A helix of HEAT 5 relative to HEAT 6, which moved Asn171, Leu174, and Ile178 to positions in which they would clash with Phe F1 of the FxFG core (Figure 6B) and so obstruct their binding to importin-β in the presence of RanGTP. This movement provides a structural explanation for how RanGTP binding could displace importin-β from FxFG-repeat nucleoporins (and probably also IBB) by introducing a conformational change into importin-β rather than competing with it directly by binding to the same (or an overlapping) site. Although the RanGTP–karyopherin-β2 structure (Chook and Blobel, 1999) was similar to that of RanGTP–importin-β (Vetter et al., 1999), sequence differences between importin-β and karyopherin-β2 prevented detailed comparison with Ib442–FF5.

Nucleoporin Repeats in Nuclear Trafficking

Interactions between importin-β and FxFG nucleoporins have been demonstrated both in vitro (Radu et al., 1995a; Rexach and Blobel, 1995; Chi and Adam, 1997; Hu et al., 1997; Shah and Forbes, 1998) and in vivo (Damelin and Silver, 2000). Moreover, importin-β deletion mutants that fail to bind these repeats fail to shuttle between cytoplasm and nucleus (Kose et al., 1999) and the addition of constructs containing FxFG repeats inhibits nuclear protein import (Shah and Forbes, 1998) (Figures 5E and 5F). Previous studies indicated that truncation mutants of importin-β lacking residues 152–352 failed to bind effectively to NPCs (Chi and Adam, 1997; Kutay et al., 1997) but these mutants also failed to bind RanGTP. The reduced nuclear protein import (Figure 5) observed with importin-β point mutants that retained RanGTP and importin-α binding, but in which the binding to FxFG nucleoporins was reduced (Figure 4), provided direct evidence for this interaction having a functional role in nuclear protein import.

Importin-β probably interacts with a range of different FxFG nucleoporins both during nuclear protein import and also in recycling to the cytoplasm. The interaction probably involves a major contribution from the FxFG cores. FxFG repeat nucleoporins are located at both faces of NPCs as well as the central transport channel (Grote et al., 1995; Stoffler et al., 1999; Rout et al., 2000), and so could facilitate the translocation of cargo-importin-β complexes through the nuclear pore by enabling importin-β to hop from one repeat to another as proposed for how NTF2 mediates the nuclear import of RanGDP (Bayliss et al., 1999) or by contributing to a Brownian affinity gating (Rout et al., 2000). It may be that directionality in this trafficking could be generated by a gradient of affinity between importin-β and different nucleoporins (see Talcott and Moore, 1999) and indeed it does appear that importin-β binds more strongly to Nup153, located on the NPC nucleoplasmic face, than to other nucleoporins (Shah and Forbes, 1998). The most straightforward way such a gradient of affinity could be generated is by the linkers between the FxFG cores making a contribution to the strength of the binding to importin-β. However, because the FxFG repeat nucleoporins function as a multidentate ligand, an affinity gradient could also be generated if the local concentration of FxFG repeats was elevated and indeed, Nup153 has

both the highest number of repeats (Rout and Wente, 1994), and also the highest affinity for importin-β. The release of importin-β from the nucleoplasmic face of the NPC by RanGTP inducing a conformational change in importin-β would then terminate translocation. In addition to weakening the interaction between nucleoporin repeats and the primary site identified in this study, such a conformational change could also generate other nucleoporin binding sites, perhaps involving other FG repeat types, involved in the export of importin-β to the cytoplasm to begin another round of import. The spectrum of interactions between different members of the importin-β family and different nucleoporins varies substantially (Pemberton et al., 1998; Seedorf et al., 1999; Talcott and Moore, 1999) and clearly not all of these interactions will involve FxFG repeat cores. Other types of interactions with nucleoporins involving, for example, zinc finger domains (Nakielny et al., 1999; Yaseem and Blobel, 1999) or GLFG repeats (Iovine et al., 1996; Radu et al., 1996b; Iovine and Wente, 1997; Powers et al., 1997) probably also contribute to the import and export of different importin-β family members. It is probable that analogous interactions with nucleoporin repeats are involved in the nucleocytoplasmic shuttling of other molecules such as, for example, β-catenin (Yokoya et al., 1999). Clearly, it will be important to define more precisely the interactions between nucleoporins and transport factors to understand more fully the mechanism by which different molecules are translocated through NPCs. However, identification of the FxFG binding site on importin-β and the construction of mutants that interfere with both this interaction and nuclear protein import, together with the likely contribution made by conformational changes in importin-β introduced by RanGTP binding, provides direct evidence for the functional importance of these interactions and a context in which the mechanism of translocation can be probed at the molecular level.

Experimental Procedures

Protein Preparations

Truncated importin-β corresponding to residues 1–442 (Ib442) was made by PCR from cloned human importin-β cDNA (Dr. S. Adam, Northwestern University, Chicago). After cloning into expression vector pET15b, sequencing confirmed that no mutations had been introduced. Ib442 protein was expressed in *E.coli* strain BL21(DE3) containing the pLysS plasmid (Studier et al., 1990) at 37°C and, after lysis and clarification, was purified by DE52 ion-exchange chromatography followed by gel filtration. The protein was over 95% pure by SDS-PAGE using Coomassie staining (Laemmli, 1970). Ib442, I178A, I178F, and I178D mutants were made using the QuikChange site-directed mutagenesis kit (Stratagene, La Jolla, CA) and sequenced to ensure that the correct mutation had been made and that no other mutations had been generated. The mutations were introduced into full-length importin-β by cutting a SalI/KpnI fragment out of the Ib442 mutant plasmids and inserting it into full-length importin-β digested with SalI/KpnI. The same mutations were introduced into S-tagged full-length importin-β using NcoI/NheI sites. Wild-type and mutant full-length importin-β were expressed in BL21(DE3) strain of *E.coli* at 37°C overnight without induction and purified using DE52 ion-exchange chromatography, phenyl-Sepharose affinity chromatography, and gel filtration. The yeast Nsp1 (Nehrbass et al., 1990) FF5 construct, corresponding to residues 497–608 with short C and N extensions (MGSS and MQA), was cloned into expression vector pMW172, expressed, and purified as described for other Nsp1p FxFG constructs (Clarkson et al., 1996). Canine Ran and Nsp1p FF18 were expressed and purified as described (Clarkson et al., 1997). Importin-α was prepared as described (Percipalle et al., 1997) except it was purified by phenyl-Sepharose chromatography.

Crystallization and Data Collection

Crystals of Ib442 complexed with FF5 were obtained by vapor diffusion using 7 μl hanging drops composed of 3 μl drop buffer, 3 μl 1–442 (2.1 mg/ml) and 1 μl FF5 (11 mg/ml). Reservoir buffer contained 1.24 M ammonium sulphate, 100 mM ammonium acetate (pH 5.5), and 50 mM DTT. Drop buffer contained 1.28–1.36 M ammonium sulphate, 200 mM ammonium acetate (pH 5.5), and 50 mM DTT. Drops were streak seeded using microcrystals of the complex and crystals were fully-grown three days after seeding. Under these conditions, neither Ib442 nor FF5 alone produced crystals, even when seeded using microcrystals of the complex. A 300 μm × 50 μm × 5 μm crystal was transferred to reservoir buffer containing 24% glycerol for less than one minute and flash-frozen at 100K. A native data set was collected at 100K using 0.933 Å wavelength radiation on beamline ID14-EH2 at ESRF (Grenoble, France) using a MAR CCD detector (Table 1) and had $P2_12_12$ symmetry. The diffraction pattern was anisotropic, with reflections past 2.8 Å along a*, but only to 3.5 Å along c*. These data were 98.5% complete to 3.4 Å, falling to 92.4% complete for 40–3.2 Å and 69.1% for 40–2.8 Å. Improved processing of the anisotropic data was achieved using a modification of MOSFLM written by Dr. H. Powell (MRC Cambridge) and was reduced using SCALA (CCP4, 1994).

Structure Solution

Molecular replacement and refinement used the CNS package (Brünger et al., 1998). Ten percent of the data was excluded during all stages of refinement for calculation of R_{free} (Brünger, 1992). We located two Ib442 chains in the asymmetric unit using residues 1–442 of the structure of $P2_1$ crystal form I of importin-β bound to the IBB domain (PBD-1qgk, Cingolani et al., 1999) as a model. We obtained similar molecular replacement solutions using the same residues from crystal type II of the IBB domain and importin-β (PDB-1qgr; Cingolani et al., 1999), but these had consistently higher R factors and lower correlation coefficients. We therefore concentrated on the solution obtained using PDB-1qgk. A model with only two Ib442 chains in the asymmetric unit together with two FF5 chains would have an expected solvent content of 66%, which, although high, was within the range commonly observed for protein crystals (Matthews, 1968). We searched exhaustively for a molecular replacement solution for a third chain, but none could be obtained that reduced the R factor. Moreover, inspection of the preliminary model indicated that there did not appear to be a sufficiently large additional volume to insert a third Ib442 chain in the asymmetric unit. After rigid body refinement based on individual HEAT repeats and group B factor refinement, the R factor of the molecular replacement solution reduced to 29.8% (R_{free} 31.5%). Positional refinement using conjugate gradient minimization, Cartesian slow cooling, and torsion-angle simulated annealing with strong noncrystallographic symmetry constraints, alternating with local rebuilding, produced a final model for the two Ib442 chains in the unit cell in which the R factor was reduced to 25.1% (R_{free} 28.3%). It was unlikely that such R factors could be obtained if our model lacked an entire Ib442 chain. Moreover, there was no obvious F_o-F_c difference density indicative of a third Ib442 chain. However, both the $2F_o-F_c$ density map obtained after solvent flipping and the F_o-F_c difference density map showed two elongated cylinders of density on the convex surface of both Ib442 chains in the asymmetric unit which we attributed to the parts of FF5 that were in close association with Ib442. One of these cylinders was located between the A helices of HEAT repeats 5 and 6, whereas the second was located between the A helices of HEAT repeats 6 and 7. The difference density between HEAT repeats 5 and 6 was stronger and had two very clear lobes indicative of large sidechains in close proximity to the surface of the Ib442 chain and which we identified with the two Phe residues of the sequence repeat core. After alternating cycles of fitting the sequence of the FF5 repeats to the density, simulated annealing refinement of the FF5 chains, and manual adjustment, the R factor was reduced to 22.5% (R_{free} 26.2%). Noncrystallographic symmetry

was applied to the repeat cores (AFSFG see Figure 1), but some linker residues were modeled as Ala when the density was not sufficiently reliable to identify sidechains unequivocally. The final structural model contained Ib442 residues 1–440 and two separate stretches of FxFG repeat (DDSKPAFSFGAAA for the primary site and AAAAAFSF for the secondary site). Table 1 gives the refinement statistics. Molecular drawings were produced using Bobscript (Esnouf, 1997) and Raster3D (Merritt and Bacon, 1997).

Biochemical Procedures

The binding of importin-α and RanGTP was assayed in PBS containing 2 mM DTT and 0.5 mg/ml BSA as a blocking agent. S-tagged wild type or mutant importin-β bound to S protein agarose (Novagen, Madison, WI) was mixed with 40 μg importin-α or RanGTP, pelleted, washed twice in PBS, and material remaining bound to the beads analyzed by SDS-PAGE. Solution binding assays using FxFG repeats coupled to CNBr-Sepharose were carried out essentially as described (Bayliss et al., 1999) using FF5, the Nsp1p construct containing five FxFG repeats. Nucleoporin-enriched extracts of rat liver nuclear envelopes were prepared as described (Buss and Stewart, 1995) and after SDS-PAGE, blotted onto nitrocellulose, blocked with 4% nonfat milk in PBS containing 0.2% Tween 20, rinsed in PBS, then incubated with 4 ng/ml S-tagged importin-β constructs. After washing in PBS, the importin-β was visualized using S protein HRP (Novagen) and ECL (Amersham, Bucks, UK). Competition assays used 34 ng/ml of FF18. Western blots were performed as described (Clarkson et al., 1997) using monoclonal antibody MAb414 (Babco, Richmond, CA) at a dilution of 1:3000 and visualized using HRP-antimouse conjugate (Sigma, Dorset, UK) followed by ECL.

Nuclear Protein Import Assay

Nuclear protein import was assayed using digitonin-permeabilized HeLa S3 cells essentially as described (Görlich et al., 1996; Kutay et al., 1997) using fluorescein-labeled BSA coupled to an NLS peptide (CGYGPKKKRKVED) as substrate or to a defective NLS peptide (CGYGPKNKRKVED) as a negative control. Purified bacterially-expressed proteins (1.2 μM importin-α, 2.25 μM Ran, and 2.7 μM NTF2) were combined in a final volume of 8 μl transport buffer (20 mM HEPES KOH [pH 7.5], 120 mM potassium acetate, 5 mM magnesium acetate, 250 mM sucrose, 0.5 mM EGTA, 5 mg/ml BSA, 0.5 mM GTP, 0.5 mM ATP, 10 mM creatine phosphate, and 0.05 mg/ml creatine kinase). Full-length importin-β and the Ile178 mutants were used at a concentration of 250 nM and were examined using identical microscope settings. In competition studies, the Nsp1p–FxFG constructs FF18 and FF5 were used at 10 μM. After 30 min, cells were fixed and examined using a MRC1024 Confocal microscope. All phase and fluorescent images were captured using 488 nm excitation and with identical laser intensity, iris, and gain settings. Ten-frame Kalman averaging was used for all images. Low-power micrographs were recorded for a number of fields in each sample and the number of cells in which fluorescent substrate had been imported into the nucleus quantitated. Approximately 100 cells were counted for each sample.

Acknowledgments

We are extremely grateful to Helen Kent for invaluable assistance in the initial part of this study and especially for engineering the Ib442 and FF5 constructs and preparing the proteins used for crystallization. We thank our colleagues in Cambridge, especially Brad Amos, Catherine Huntington, Richard Grant, Rosanna Baker, Andrew Leslie, Jade Li, Roger Williams, Kiyoshi Nagai, and Tony Mills, for their valuable advice, comments, and criticisms; Ed Mitchell and Soichi Wakatsuki for assistance collecting data at ESRF (Grenoble); and Steve Adam and Ed Hurt for supplying cDNA. This work was supported in part by HFSP RG270/1998.

Received February 28, 2000; revised May 16, 2000.

References

Adam, S.A. (1999). Transport pathways of macromolecules between the nucleus and the cytoplasm. Curr. Opin. Cell Biol. *11*, 402–406.

Bayliss, R., Ribbeck, K., Akin, D., Kent, H.M., Feldherr, C.M., Görlich, D., and Stewart, M. (1999). Interaction between NTF2 and FxFG-containing nucleoporins is required to mediate nuclear import of RanGDP. J. Mol. Biol. *293*, 579–593.

Bonifaci, N., Moroianu, J., Radu, A., and Blobel, G. (1997). Karyopherin b2 mediates nuclear import of a mRNA binding protein. Proc. Natl. Acad. Sci. USA *94*, 5055–5060.

Brünger, A.T. (1992). Free R value: a novel statistical quality for assessing the accuracy of crystal structures. Nature *355*, 472–474.

Brünger, A.T., Adams, P.D., Clore, G.M., DeLano, W.L., Gros, P., Grosse-Kunstleve, R.W., Jiang, J.S., Kuszewski, J., Nilges, M., Pannu, N.S., et al. (1998). Crystallography and NMR system: a new software suite for macromolecular structure determination. Acta Crystallogr. *50*, 905–921.

Buss, F., and Stewart, M. (1995). Macromolecular interactions in the nucleoporin p62 complex of rat nuclear pores. J. Cell Biol. *128*, 251–261.

Chi, N.C., and Adam, S.A. (1997). Functional domains in nuclear import factor p97 for binding the nuclear localization sequence receptor and the nuclear pore. Mol. Biol. Cell *8*, 945–956.

Chook, Y.M., and Blobel, G. (1999). Structure of the nuclear transport complex karyopherin-β2-Ran GppNHp. Nature *399*, 230–237.

Cingolani, G. Petose, C., Weis, K., and Müller C. W. (1999). Structure of importin-β bound to the IBB domain of importin-α. Nature *399*, 221–229.

Clarkson, W.D., Kent, H.M., and Stewart, M. (1996). Separate binding sites on nuclear transport factor 2 (NTF2) for GDP-Ran and the phenylalanine-rich repeat regions of nucleoporins p62 and Nsp1p. J. Mol. Biol. *263*, 517–524.

Clarkson, W.D., Corbett, A.H., Paschal, B.M., Kent, H.M., McCoy, A. J., Gerace, L., Silver, P.A., and Stewart, M. (1997). Nuclear protein import is decreased by engineered mutants of nuclear transport factor 2 (NTF2) that do not bind GDP Ran. J. Mol. Biol. *272*, 716–730.

CCP4 (1994). Collaborative Computational Project, Number 4. The CCP4 suite: programs for protein crystallography. Acta Crystallog. *50*, 760–763.

Damelin, M., and Silver, P.A. (2000). Mapping interactions between nuclear transport factors in living cells reveals pathways through the nuclear pore complex. Mol. Cell, *5*, 133–140.

Esnouf, R.M. (1997). An extensively modified version of MolScript that includes greatly enhanced colouring capabilities. J. Mol. Graph. Model. *15*, 132–136.

Feldherr, C.M., Kallenbach, E., and Schultz, N. (1984). Movement of karyophilic protein through the nuclear pores of oocytes. J. Cell Biol. *99*, 2216–2222.

Finlay, D.R., and Forbes, D.J. (1990). Reconstitution of biochemically altered nuclear pores: transport can be eliminated and restored. Cell *60*, 17–29.

Görlich, D. (1998). Transport into and out of the cell nucleus. EMBO J. *17*, 2721–2727.

Görlich, D., and Kutay, U. (1999). Transport between the cell nucleus and the cytoplasm. Ann. Rev. Cell Devel. Biol. *15*, 607–660.

Görlich, D., Panté, N., Kutay, U., Aebi, U., and Bischoff, F.R. (1996). Identification of different roles for RanGDP and RanGTP in nuclear protein import. EMBO J. *15*, 5584–5594.

Greenfield, N., and Fasman, G. (1969). Computed circular dichrosim spectra for the evaluation of protein conformation. Biochemistry, *68*, 4108–4116.

Grote, M., Kubitscheck, U., Reichelt, R., and Peters, R. (1995). Mapping of nucleoporins to the centre of the nuclear pore complex by post-embedding immunogold electron microscopy. J. Cell Sci. *108*, 2963–2972.

Hu, T., Guan, T., and Gerace, L. (1997). Molecular and functional characterisation of the p62 complex, an assembly of nuclear pore complex proteins. J. Cell Biol. *134*, 589–601.

Iovine, M.K., and Wente, S.R. (1997). A nuclear export signal in Kap95p is required for both recycling the import factor and interaction with the nucleoporin GLFG repeat regions of Nup116p and Nup100p. J. Cell Biol *137*, 797–811.

Iovine, M.K., Watkins, J.L., and Wente, S.R. (1996). The GLFG repetitive region of the nucleoporin Nup116p interacts with Kap95p, an essential yeast nuclear import factor J. Cell Biol. *131*, 1699–1713.

Kehlenbach, R.H., Dickmanns, A., Kehlenbach, A., Guan, T., and Gerace, L. (1999). A role for RanBP1 in the release of CRM1 from the nuclear pore complex in a terminal step of nuclear export. J. Cell Biol. *145*, 645–657.

Kose, S., Imamoto, N., Tachibana, T., Yoshida, M., and Yoneda, Y. (1999). Beta-subunit of nuclear pore-targeting complex (importin-β) can be exported from the nucleus in a Ran-independent manner. J. Biol. Chem. *274*, 3946–3952.

Kutay, U., Izaurralde, E., Bischoff, F.R., Mattaj, I.W., and Görlich, D. (1997). Dominant-negative mutants of importin-β block multiple pathways of import and export through the nuclear pore complex. EMBO J. *16*, 1153–1163.

Laemmli, U.K. (1970). Cleavage of structural proteins during the assembly of the head of bacteriophage T4. Nature *227*, 680–685.

Matthews, B.W. (1968). The solvent content of protein crystals. J. Mol. Biol. *33*, 491–497.

Melchior, F., and Gerace, L. (1998). Two-way trafficking with Ran. Trends Cell. Biol. *5*, 175–179.

Merritt, E.A., and Bacon, D.J. (1997). Raster3D photorealistic molecular graphics. Meth. Enzymol. *277*, 505–524.

Nakielny, S., and Dreyfuss, G. (1999). Transport of proteins and RNAs in and out of the nucleus. Cell *99*, 677–690.

Nakielny, S., Shaikh, S., Burke, B., and Dreyfuss, G. (1999). Nup153 is an M9-containing mobile nucleoporin with a novel Ran-binding domain. EMBO J. *18*, 1982–1995.

Nehrbass, U., Kern, H., Mutvei, A., Horstmann, H., Marshallsay, B., and Hurt, E.C. (1990). NSP1: a yeast nuclear envelope protein localized at the nuclear pores exerts its essential function by its carboxy-terminal domain. Cell *61*, 979–989.

Paschal, B.M., and Gerace, L. (1995). Identification of NTF2, a cytosolic factor for nuclear protein import that interacts with nuclear pore complex protein p62. J. Cell Biol. *129*, 925–937.

Pemberton, L.F., Blobel, G., and Rosenblum, J.S. (1998). Transport routes through the nuclear pore complex. Curr. Opin. Cell Biol. *10*, 392–399.

Percipalle, P., Clarkson, W.D., Kent, H.M., Rhodes, D., and Stewart, M. (1997). Molecular interactions between the importin-α/β heterodimer and proteins involved in vertebrate nuclear protein import. J. Mol. Biol. *266*, 722–732.

Powers, M.A., Forbes, D.J., Dahlberg, J.E., and Lund, E. (1997). The vertebrate GLFG nucleoporin, Nup98, is an essential component of multiple RNA export pathways. J. Cell Biol. *136*, 241–250.

Radu, A., Blobel, G., and Moore, M.S. (1995a). Identification of a protein complex that is required for nuclear protein import and mediates docking of import substrate to distinct nucleoporins. Proc. Natl. Acad. Sci. USA *92*, 1769–1773.

Radu, A., Moore, M.S., and Blobel, G. (1995b). The peptide repeat domain of nucleoporin Nup98 functions as a docking site in transport across the nuclear pore complex. Cell *81*, 215–222.

Rexach, M., and Blobel, G. (1995). Protein import into nuclei: association and dissociation reactions involving transport substrate, transport factors, and nucleoporins. Cell *83*, 683–692.

Rout, M.P., and Wente, S.R. (1994). Pores for thought: nuclear pore complex proteins. Trends Cell Biol. *4*, 357–365.

Rout, M.P., Aitchison, J.D., Suprapto, A., Hjertaas, K., Zhao, Y., and Chait, B.T. (2000). The yeast nuclear pore complex. Composition, architecture, and transport mechanism. J. Cell Biol. *148*, 635–652.

Seedorf, M., Damelin, M., Kahana, J., Taura, T., and Silver, P.A. (1999). Interactions between a nuclear transporter and a subset of nuclear pore complex proteins depend on Ran GTPase. Mol. Cell. Biol. *19*, 1547–1557.

Shah, S., Tugendreich, S., and Forbes, D. (1998). Major binding sites for the nuclear import receptor are the internal nucleoporin Nup153 and the adjacent nuclear filament protein Tpr. J. Cell Biol. *141*, 31–40.

Shah, S., and Forbes, D.J. (1998). Separate nuclear import pathways converge on the nucleoporin Nup153 and can be dissected with dominant negative inhibitors. Curr. Biol. *8*, 1376–1386.

Stewart, M., and Rhodes, D. (1999). Switching affinities in nuclear trafficking. Nature Struct. Biol. *6*, 301–304.

Stoffler, D., Fahrenkrog, B., and Aebi, U. (1999). The nuclear pore complex: from molecular architecture to functional dynamics. Curr. Opin. Cell Biol. *11*, 391–401.

Studier, F.W., Rosenburg, A.H., Dunn, J.J., and Dubedorff, J.W. (1990). Use of T7 RNA polymerase to direct expression of cloned genes. Meth. Enzymol. *185*, 60–89.

Talcott, B., and Moore, M.S. (1999). Getting across the nuclear pore complex. Trends Cell Biol. *9*, 312–318.

Vetter, I., Arndt, A., Kutay, U., Görlich, D., and Wittinghofer, A. (1999). Structural view of the Ran-importin β interaction at 2.3 Å resolution. Cell *97*, 635–646.

Yaseem, N.R., and Blobel, G. (1999). GTP hydrolysis links initiation and termination of nuclear import on the nucleoporin Nup358. J. Biol. Chem. *274*, 26493–26502.

Yokoya, F., Imamoto, N., Tachibana, T., and Yoneda, Y. (1999). β-catenin can be transported into the nucleus in a Ran-unassisted manner. Mol. Biol Cell. *10*, 1119–1131.

Protein Data Bank Accession Code

The atomic coordinates of the Ib442–FF5 crystal described in this paper have been deposited in the Protein Data Bank with accession code 1F59.